Materials Research. 2014; 17(2): 346-351
DOI: http://dx.doi.org/10.1590/S1516-14392014005000019

Radiation Induced Synthesis of In_2O_3 Nanoparticles - Part 1: Synthesis of In_2O_3 Nanoparticles by Sol-gel Method Using Un-irradiated and γ-Irradiated Indium Acetate

*Ajayb Al-Resheedi[a], Norah Saad Alhokbany[a], Refaat Mohammed Mahfouz[b]**

[a]*Department of Chemistry, College of Science, King Saud University – KSU, Riyadh 11451, P.O. Box 2455, Kingdom of Saudi Arabia*
[b]*Chemistry Department, Faculty of Science, Assiut University – AUN, Assiut 71516, Egypt*

Received: March 31, 2013; Revised: November 13, 2013

Pure phase of In_2O_3 nanoparticles were synthesized by sol-gel method in non-aqueous medium using un-irradiated and γ-irradiated indium acetate precursors. The as-prepared In_2O_3 nanoparticles were characterized by XRD, FT-IR, SEM, TEM and TG techniques. The results showed that pre-irradiation to indium acetate with 10^2 KGy γ-ray absorbed dose has significant effects on the shape and size of the as-synthesized In_2O_3 nanoparticles. In case of un-irradiated precursor, the SEM images show agglomerated and disordered spherical nanoparticles. In γ-irradiated case the particles showed coral-like structure. The as-synthesized In_2O_3 nanoparticles prepared using γ-irradiated precursor showed higher thermal stability compared with those prepared using un-irradiated one. The results were discussed in view of the role of γ-irradiation on the morphology and thermal behavior of In_2O_3 nanoparticles.

Keywords: *-irra, γ, In2O3, sol-gel process*

1. Introduction

In_2O_3 is an important n-type semi-conductor with a wide band gap of potential use in optoelectronic devices and gas sensing applications[1-3]. In_2O_3 has two crystalline phases: Cubic In_2O_3 (c- In_2O_3) and hexagonal In_2O_3 (h-In_2O_3) with cubic phase as favorable phase for industrial applications[4,5]. Several routes such as chemical vapor deposition (CVD)[6], sol-gel[7], solution-phase growth[8] and solid state decomposition[9] have been employed for preparation of In_2O_3 nanoparticles. Pre-irradiation of the precursors with high energy charged particles (electrons, ions) as well as X-rays and γ-rays can aid in the synthesis of nanoparticles by sol-gel and by solid state thermal decomposition methods. Whereas the un-irradiated precursors are commonly used, the control provided by the broad range of dose and dose rate might offer advantages in the fine-tuning of the size and morphology of the nanoparticles[10-13]. Irradiation effects on the preparation of In_2O_3 nanoparticles were scanty investigated and to the best of our knowledge only one publication dealing with radiation induced synthesis of In_2O_3 nanoparticles is reported[14].

In the present work, we started a comprehensive study on the radiation-induced synthesis of In_2O_3 nanoparticles by both sol-gel and solid-state thermal decomposition methods. Several influencing factors including variation of γ-ray absorbed dose, addition of surfactants, and variation of the used indium precursors were thoroughly investigated.

In our first submission, we started with un-irradiated and γ-irradiated indium acetate with 10^2 KGy γ-ray absorbed dose as precursors for preparation of In_2O_3 nanoparticles by sol-gel method.

*e-mail: rmhfouz@science.au.edu.eg

2. Experimental

2.1. *Synthesis of In_2O_3 nanoparticles*

All the chemicals used in this study were of analytical grade, purchased from Sigma-Aldrich and used without further purification

0.1 mole of both un-irradiated and 10^2 KGy absorbed dose of γ-irradiated anhydrous indium acetate (InAc) were included in two separate round flasks at room temperature. 0.3 mole of anhydrous benzyl alcohol was added dropwise to each flask with good stirring until white gels were formed. 100 mg of sodium dodecyl sulphate were added to each gel with stirring for ≈5 min. The two gels were subjected to thermal treatments at different calcination temperatures for different time intervals. At each calcination stage, the gel was investigated using FT-IR and TG techniques to follow the formation of In_2O_3 nanoparticles as final product.

2.2. *Characterization*

X-ray powder diffraction patterns (XRD) were recorded on siemens JDX-3530 X-ray diffractometer equipped with graphite monochromatized Cu Kα radiation (λ= 1.54178 Å). FT-IR measurements were recorded as KBr pellets in the range of 4400-400 cm^{-1} on Perkin- Elemer FT-IR spectrophotometer. TEM images were captured on JOEL JEM 2010 TEM. SEM images were recorded using HITACHIS-4800 SEM. TG measurements were recorded on Perkin-Elemer TG A7 thermogravimetric analyzer in the range of 30-1000 °C. The sample weight was 10.0 ± 0.1 mg with heating rate of 10 °C/min.

For irradiation, samples were encapsulated under vacuum in glass vials and exposed to successively increasing doses of radiation at constant intensity using a Co-60

γ-ray Cell 220 (Nordion INT-INC, Ontario, Canada). The exposure dose was attenuated to be 10^4KGy/h in order to save irradiation time. The source was calibrated against a Fricke ferrous sulphate dosimeter and the absorbed doses in the irradiated samples were calculated by applying appropriate corrections on the basis of photon mass attenuation and the energy absorption coefficients for the sample and the dosimeter solutions. After irradiation the samples were stored at room temperature for 24 h before analysis.

3. Results and Discussion

Figure 1 shows typical TG curves of the gel prepared using un-irradiated InAc precursor. Decomposition of the gel proceeds through three major steps. The first decomposition step was in the range of 50-110 °C, the second weight loss step was in the range of 520-270 °C and the third weight loss was in the range of 280-350 °C. The total experimental weight loss percentage (≈75%) was in good agreement with the percentage (74%) expected theoretically assuming release of three benzyl alcohol molecules, with the formation of In2O3 as final solid residue. The decomposition of the gel prepared using γ-irradiated InAc precursor proceeds by the same thermal behaviour as with the un-irradiated one.

Figure 2 shows FT-IR of the gels formed using un-irradiated and γ-irradiated InAc precursors before and after thermal oxidation treatments at 200 and at 400 °C calcinations temperatures for 5 hours respectively. The Figure 2 shows systematic decrease in the intensity of the absorption bands characteristic for benzyl alcohol molecules. Complete annealing of the gel and formation of In_2O_3 nanoparticles was achieved by calcination at 400 °C for 5 hours as shown in Figure 2.The figure show the characteristic bands attributed to In-O phonon mode of vibration of cubic In_2O_3 nanoparticles in the range of 400-800 cm^{-1}[15]. The chemisorbed H_2O and CO_2 molecules on the surface of In_2O_3 could be easily detected by recording the bands appeared in the range of 3400-3500 cm^{-1} and 1700-1600 attributed to νOH and νC=O respectively.

XRD patterns of the as-prepared samples for both un-irradiated and γ-irradiated InAc with 10^2 KGy calcined at 200 °C for 5 hours show diffraction lines indexed as mixed phase of cubic and hexagonal In_2O_3 for both un-irradiated and γ-irradiated InAc[16].

The diffraction lines for the samples calcined at 400 °C for 5 hours are all indexed to pure body centered cubic (bcc) structure of In_2O_3 (JCPDS Card No. 06-0416) as shown in Figure 3. No others impurity peaks were detected in the pattern which reveal the high phase purity of the sample. In addition, the EDS analyses also indicate only indium and oxygen as constituent's elements. The broadening of the obtained lines confirm nanocrystalline nature of the phase. However, in case of γ-irradiation precursor, the XRD pattern shows more broadening in the width of diffraction lines. This broadening leads to a decrease in the lattice dimensions due to the radiation damage induced by γ-irradiation in the host lattice of InAc precursor. This behavior was confirmed by calculating the particle size of In_2O_3 nanoparticles by using of the Deby-Sherrer formula[17].

$$t = \frac{0.89\ \lambda}{\beta \cos \theta_B} \quad (1)$$

where λ is the wavelength (in Angstrom), β is the broadening of the diffraction peaks (in radians) or full width at half maximum (FWHM), θ_B is the Bragg diffraction angle. The calculated average particle size of In_2O_3 nanoparticles was estimated to be in the ranges of (10-20) and (10-15) nm in case of un-irradiated and γ-irradiated precursors respectively.

SEM images of In_2O_3 nanoparticles obtained by using of un-irradiated and γ-irradiated InAc precursors are shown in Figure 4. Both images display the nanocrystalline nature of the as-prepared powders, with significant differences in the shape and size of the as-prepared In_2O_3 nanoparticles as a result of γ-irradiation. In case of un-irradiated precursor, the SEM images show agglomerated and disordered spherical nanoparticles. In γ-irradiated case the particles showed coral-like structure. TEM images of the as-prepared In_2O_3 nanoparticles showed also significant changes in the morphology of the particles prepared using un-irradiated and γ-irradiated precursors. In case of γ-irradiation, in contrast to the agglomerated cubic In_2O_3 obtained using un-irradiated

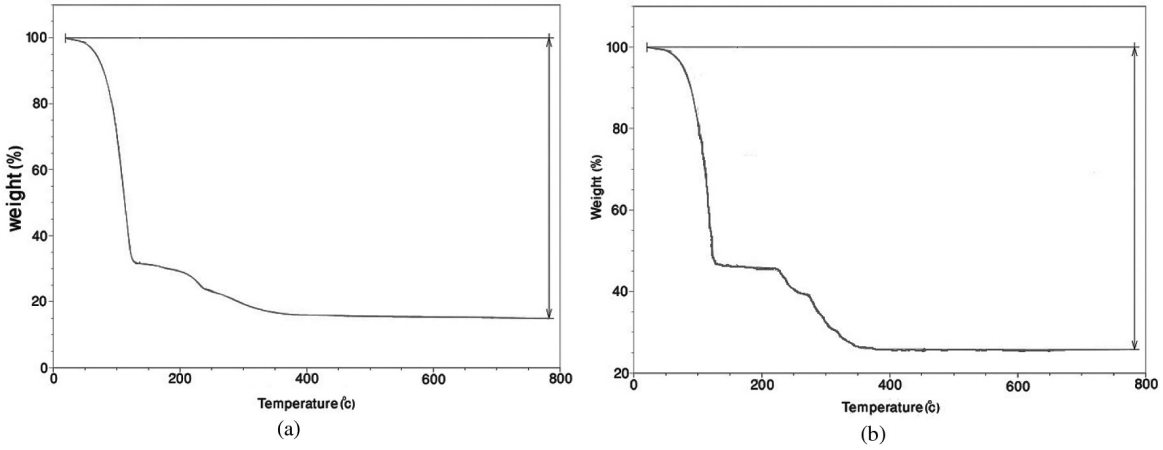

Figure 1. Typical TG curves of the gels prepared using. (a) un-irradiated InAc; (b) γ-irradiated InAc (10^2 KGy).

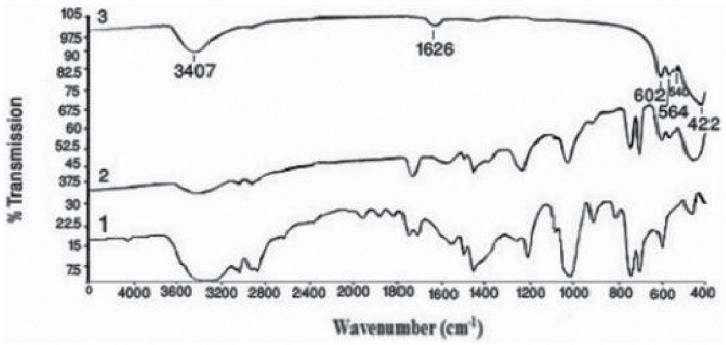

(a)

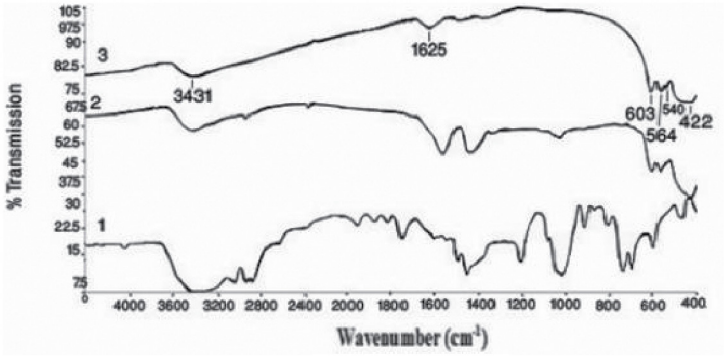

(b)

Figure 2. FT-IR of the gels prepared using (a) un-irradiated and (b) γ-irradiated (10^2 KGy) InAc precursors. 1-without thermal treatment; 2- calcined at 200 °C for 5 hours; 3- calcined at 400 °C for 5 hours.

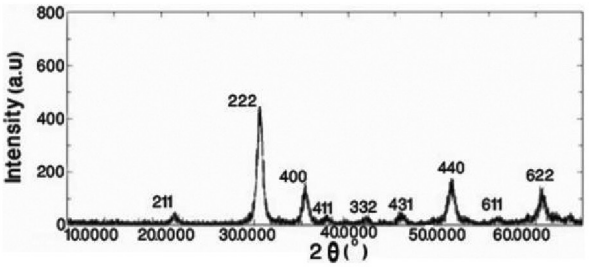

(a)

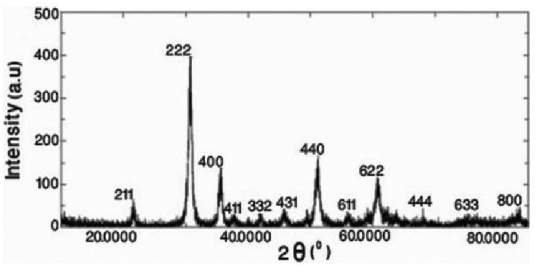

(b)

Figure 3. The XRD patterns of the samples calcined at 400 °C for 5 hours. (a) un-irradiated and (b) γ-irradiated InAc precursors.

precursors, the image obtained for γ-irradiated precursor showed blocks of agglomerated nanocubes (primary of nanocrystallites) with big holes between these blocks These nanocubes exhibit different orientation compared with those prepared by un-irradiated precursor. The nanocubes in case of ɣ irradiated precursor are preferentially oriented along 222 planes as was confirmed by XRD pattern of In_2O_3 obtained using γ-irradiated precursor. The average particle size (≈ 10 nm) was estimated to be quite smaller than the value calculated using un-irradiated precursor (≈ 15 nm).

Thermal stability of In_2O_3 nanoparticles were examined to illustrate the role of γ-irradiation on the thermal stability of the as-prepared In_2O_3 nanoparticles. In general, the In_2O_3 nanoparticles prepared using γ-irradiated InAc precursor showed higher thermal stability compared with those prepared using un-irradiated InAc. The weight loss in the temperature range of 50-600 °C was attributed to release of adsorbed water and volatile carbonate from the surface of In_2O_3 nanoparticles. Starting by 650 °C the TG curve for In_2O_3 nanoparticles prepared by un-irradiated InAC precursor show continuous weight loss due to degradation process. No detectable weight loss was recorded in the TG curves for In_2O_3 nanoparticles of γ-irradiated InAc up to 800 °C the results are shown in Figure 5.The stability of In_2O_3 nanoparticles prepared using un-irradiated precursor up to 800 °C clearly indicate that these particles can act as molten salts in the temperature range of 600 to 800 °C.This is the first report of the behavior of In_2O_3 as molten salt in the temperature range of 600 to 800 °C.

Figure 6 shows the RT-PL spectra of the as-synthesized In_2O_3 nanoparticles. While exciting the sample with 266 nm, a strong emission at 383 nm and a weak emission at 650 nm

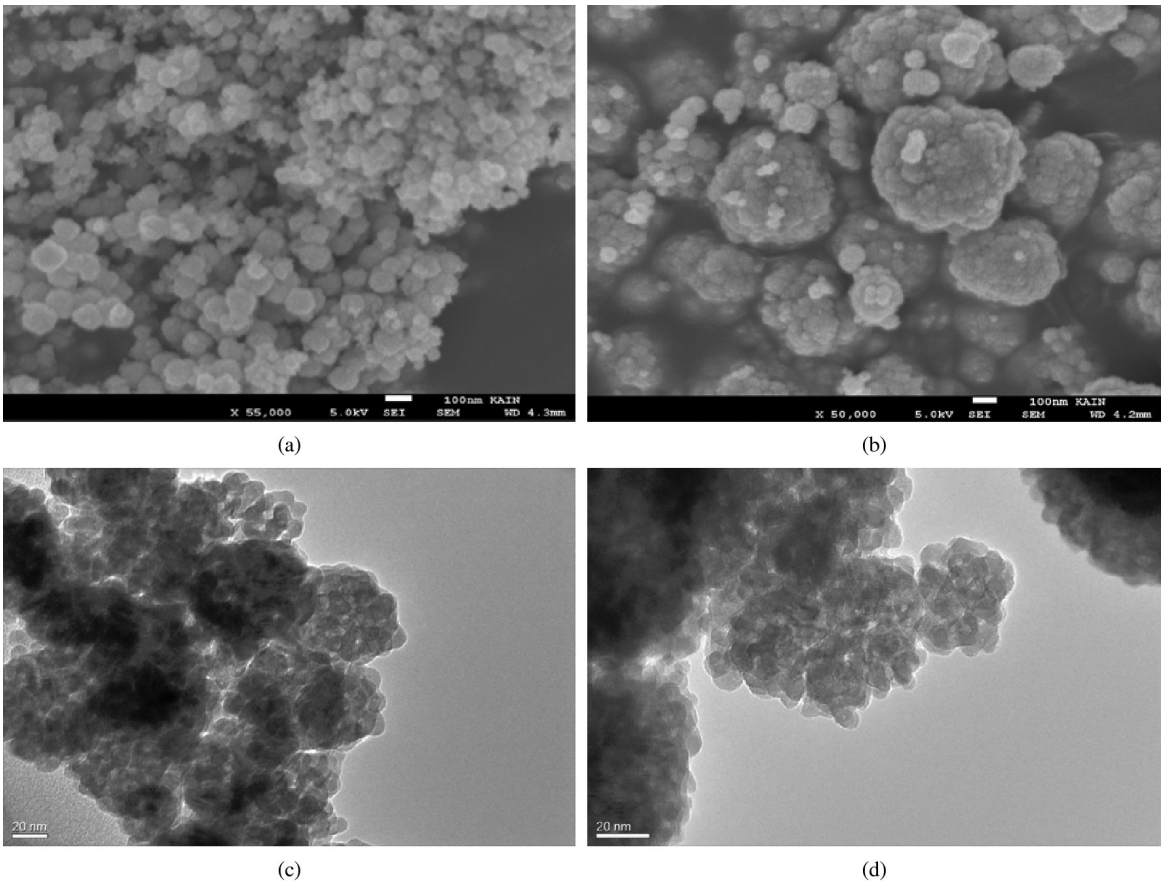

Figure 4. SEM and TEM images of In_2O_3 nanoparticles obtained by using of un-irradiated (a, c) and γ-irradiated (b, d) InAc precursors.

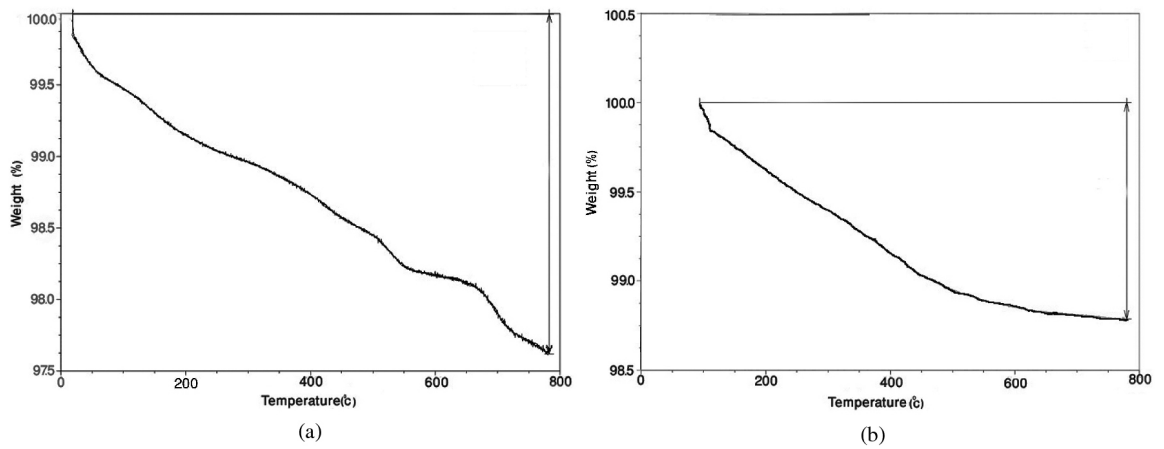

Figure 5. Typical TG curves of the as-synthesized In_2O_3 nanoparticles. (a) un-irradiated and (b) γ-irradiated InAc precursors.

were recorded. It is well known that bulk In_2O_3 cannot emit light, while its nanostructure can emit visible and UV light. The PL emission by nanocrystals in the visible range was mainly attributed to creation of oxygen vacancies. These oxygen vacancies induce the formation of new energy levels in the band gap which facilitate the electronic transitions between valence band and conduction bands[18].

3.1. *Role of irradiation*

Upon irradiation with Co-60 γ-ray source, the photoelectric effect is the main mode of interaction of γ-ray with indium atom. In this way, stable molecules (M) are converted into solvated electrons (e) and high reactive free radicals (M^+).In solid samples, the radiation effect is dominated by direct ionization of the material whereas for

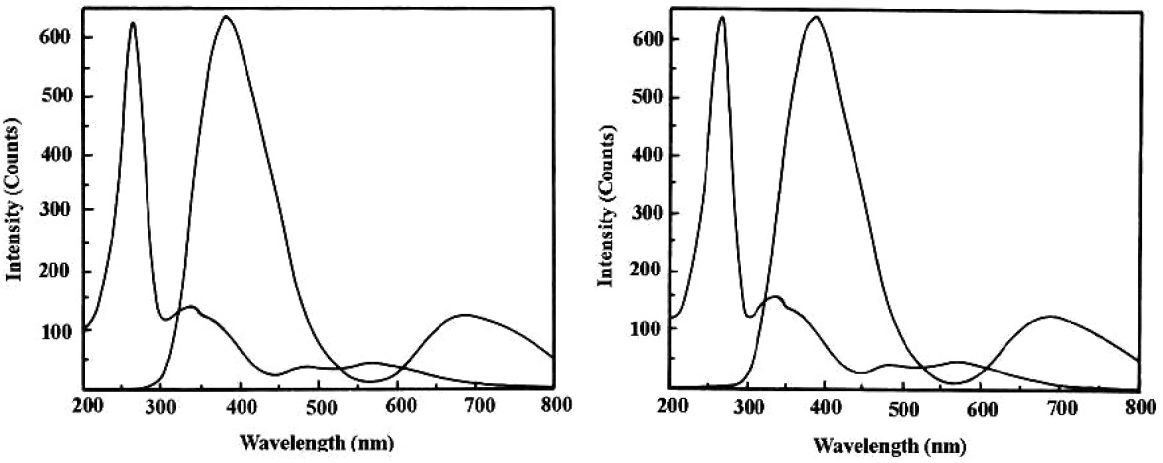

Figure 6. The RT-PL spectra of the as-synthesized In_2O_3 nanoparticles. (a) un-irradiated and (b) γ-irradiated InAc precursors.

aqueous liquids the reaction with radical species such as OH^- or solvated electrons is the dominant mechanism for damage to a solute. The solvated electrons are trapped in the interstitials and vacancies positions in the host lattice of indium acetate unit cell and not allowed to interact with anhydrous benzyl alcohol moiety. These crystal defects could lead to point defect (anion Frenkel defect where O^{2-} is the interstitial ion), defect clusters and extended defects. As a result of these events, impurity and non-stoichiomertric centers are created. Accordingly some kinds of modifications either in the morphology of the as-synthesized nanoparticles or in the course of thermal decomposition behavior of γ-irradiated materials may be generated[19]. From crystallographic point of view, when unit cell is exposed to γ-irradiation , the atoms may be disturbed from the equilibrium positions. Accordingly, the scattering action changes so that the structure factor becomes different. The lattice parameters was calculated from 222 plane by using of the formula

$$\frac{1}{d^2} = \frac{h^2 + k^2 + l^2}{a^2} \quad (2)$$

where d is the d-spacing parameter, and *hkl* are Miller indices (222) plane. The calculated parameter, a , in case of γ-irradiation

(10.05 Å) was estimated to be less than the estimated value (10.09 Å) using un-irradiated precursor. The two values are in good agreement with the reported value of 10.11 Å (international center for diffraction data card no. 04-015-4061)

4. Conclusion

In_2O_3 nanoparticles were prepared by sol-gel method in non-aqueous medium using anhydrous benzyl alcohol and indium acetate as precursor. Pre-irradiation of indium acetate with 10^2 KGy absorbed γ-ray dose led to significant changes in the morphology and thermal properties of the as-synthesized In_2O_3 nanoparticles. Further studies concerning the effects of varying γ-ray dose on the preparation of In_2O_3 nanoparticles and their applications as sensors are in progress in our laboratory.

Acknowledgments

This research project was supported by a grant from the research center of the center for the female scientific and medical colleges in King Saud University.

References

1. Murali A, Barve A, Leppert VJ, Risbud SH, Kennedy IM and Lee H. Synthesis and Characterization of Indium Oxide Nanoparticles. *Nano Letters.* 2001; 1(6):287-289. http://dx.doi.org/10.1021/nl010013q
2. Li C, Zhang D, Liu X, Han S, Tang T, Han J and Zhou C. In_2O_3 nanowires as chemical sensors . *Applied Physics Letters.* 2003; 82:1613. http://dx.doi.org/10.1063/1.1559438
3. Xu JQ, Wang XH, Wang GQ, Han JJ and Sun YA. Solvothermal synthesis of In_2O_3 nanocrystal and its ethanol sensing mechanism *Electrochemical and Solid State Letters.* 2006; 9(11):103-107. http://dx.doi.org/10.1149/1.2335943
4. Wang X, Zhang M, Liu J, Luo T and Qian Y. Shape- and phase-controlled synthesis of In_2O_3 with various morphologies and their gas-sensing properties. *Sensors and Actuators B*: Chemical. 2009; 137(1):103-110. http://dx.doi.org/10.1016/j.snb.2008.11.027
5. Oprea A, Gurlo A, Bârsan N and Weimar U. Transport and gas sensing properties of In_2O_3 nanocrystalline thick films: A Hall effect based approach. *Sensors and Actuators B*: Chemical. 2009; 139(2):322-328. http://dx.doi.org/10.1016/j.snb.2009.03.002
6. Ping Shen X, Jiang Liu H, Fan X, Jiang Y, Ming Hong J and Xu Z. Construction and photoluminescence of In_2O_3 nanotube array by CVD-template method. *Journal of Crystal*

Growth. 2005; 276(3-4):471-477. http://dx.doi.org/10.1016/j.jcrysgro.2004.11.394

7. Du J, Yang M, Nam Cha S, Rhen D, Kang M and Kang DJ. Indium Hydroxide and Indium Oxide Nanospheres, Nanoflowers, Microcubes, and Nanorods: Synthesis and Optical Properties. *Crystal Growth & Design.* 2008; 8(7):2312-2317. http://dx.doi.org/10.1021/cg701058v
8. Zhu P, Wu W, Zhou J and Zhang W. Preparation of size-controlled In_2O_3 nanoparticles. *Applied Organometallic Chemistry*. 2007; 21(10):909-912. http://dx.doi.org/10.1002/aoc.1300
9. Dodd A. Synthesis of indium oxide nanoparticles by solid state chemical reaction. *Journal of Nanoparticle Research*. 2009; 11(8):2171-2177. http://dx.doi.org/10.1007/s11051-009-9707-x
10. Maurizot MS, Mostafavi M, Douki T and Belloni J, editors. Radiation chemistry from basics to applications in material and life sciences. Edp Sciences; 2008.
11. Chmieleki AG, editor. *Emerging applications of radiation in nanotechnology*. Vienna: IAEA; 2005. IAEA TECDDOC-1438.
12. Gerasimov GY. Radiation methods in nanotechnology. *Journal of Engineering Physics and Thermophysics*. 2011; 84(4):947-963. http://dx.doi.org/10.1007/s10891-011-0554-0
13. Chmielewski AB, Chmielewska DK, Michalik J and Sampa MH. Prospects and challenges in application of gamma, electron and ion beams in processing of nanomaterials. *Nuclear Instruments and Methods in Physics Research*. 2007; B265(1):339-346. http://dx.doi.org/10.1016/j.nimb.2007.08.069
14. Mahfouz RM, Al-Ahmari Sh, Al-Fawaz A, Al-Othman Z, Kh-Warad KhI and Siddiqui MR. Kinetic Analysis for Non-isothermal Decomposition of Unirradiated and γ-Irradiated Indium Acetyl Acetonate. *Materials Research.* 2011; 14(1):7-10. http://dx.doi.org/10.1590/S1516-14392011005000009
15. Nyquist RA and Kagel RO. *Infrared Spectra of Inorganic Compounds.* New York: Academic Pres; 1971. p. 208.
16. Fan Y, Wang S and Sun ZX. In_2O_3 hollow spheres: One-step solvothermal synthesis and gas sensing properties. *Materials Chemistry and Physics*; 2012; 134(1):93-97. http://dx.doi.org/10.1016/j.matchemphys.2012.02.034
17. Chandradass J, Dong SD, Chandradass J, Bae DS, Kim KH and Hyeonkim K. A simple method to prepare indium oxide nanoparticles: Structural, microstructural and magnetic properties. Advanced Powder *Technology.* 2011; 22(3):370-374. http://dx.doi.org/10.1016/j.apt.2010.05.006
18. Cao BX, Zhao Y and Wu Z. Synthesis and characterization of In_2S_3 nanoparticles. *Journal of Alloys and Compounds.* 2009; 472(1-2):325-327. http://dx.doi.org/10.1016/j.jallcom.2008.04.047
19. Mahfouz RM, Monshi MAS and Abd El-Salam NM. Kinetics of the thermal decomposition of γ-irradiated gadolinium acetate. *Thermochimica Acta.* 2002; 383(1-2):95-101. http://dx.doi.org/10.1016/S0040-6031(01)00682-7